11th International Symposium on Magnetic Bearings
August 26-29, Nara, Japan

OBSERVER-BASED UNBALANCE COMPENSATION IN LQ CONTROL OF AMBS

Rafał P. Jastrzębski
Dept. of Electrical Eng., Lappeenranta Univ. of Technology, Lappeenranta 53851 Finland
rjastrz@lut.fi

Riku Pöllänen
Dept. of Electrical Eng., Lappeenranta Univ. of Technology, Lappeenranta 53851 Finland
riku.pollanen@lut.fi

ABSTRACT
In this work, a model-based linear-quadratic controller with an optimal observer-based unbalance force rejection control for variable speed magnetically suspended rotors is presented. The unbalance force rejection control is considered in two variants. In the first one, the unbalance forces are canceled and the system can maintain an accurate reference rotor position. This variant results in low measured vibration amplitudes. In the second one, the magnetic force vibrations are canceled and the rotor spins about its principal axis of inertia within the bearing clearance. The control currents and energy usage are minimal, and the vibrations are slightly decreased. Both cases are designed as a periodic disturbance observer. Simulations for the variable speed and an experimental evaluation at the constant speed are presented.

INTRODUCTION
In a spinning rotor there are always some sinusoidal disturbance forces acting on the rotor. These forces are caused by the mass unbalance, which can be described as a discrepancy between the fixed axis of rotation (usually, the assumed axis of geometry of the rotor) and the principal axis of inertia. Apart from an unbalance, all other discrepancies and imperfections, which make the system non-axisymmetrical, may cause additional harmonic disturbances. The resulting disturbance forces are proportional to the square of the rotational speed.

The unbalance compensation in the AMB applications is referred to as an unbalance force rejection control (UFRC). In AMBs, the use of active control and the possibility of changing the stiffness and damping provide better capabilities to deal with the unbalance than in the traditional bearings. Basically, a compensation mechanism is synchronized with the rotational speed. It injects compensating harmonic signals of proper amplitudes, frequencies, and phases to the control system. In general, it is possible either to cancel the effect of the unbalance forces on the rotor position and position vibrations or to cancel the effect of the unbalance forces on the control currents and the magnetic force vibrations.

The literature on AMBs provides different UFRC methods. An adaptive feedforward compensation and discrete Fourier transform are applied in [1]. Grochmal and Lynch [2] suggest the reduced-order disturbance observer with the observer gains computed analytically (based on the desired location of eigenvalues) and scheduled according to the rotational speed. The interesting approach is presented in [3], where the observer-based unbalance compensator performs an on-line identification of the physical characteristics of the unbalance and uses the result to tune the compensator. The compensation technique presented in [3] works under varying rotor speed. Many other compensation methods are also available as listed in [1] and [4].

This work presents an optimal full-order observer-based UFRC with the parameters scheduled according to the rotational speed. The proposed solution utilizes the centralized controller for multiple-input multiple-output (MIMO) radial suspension with the actively controlled first flexible mode. The compensation is considered in two variants. In the first one, the unbalance forces (position vibrations) are canceled. In the second one, the magnetic force vibrations are canceled. In the case of unbalance force cancellation, two different design methods with equivalent performance are employed and compared with respect to their robust stability. For better comparison, both the design methods are used in such a way that they result in the same closed-loop eigenvalues.

CONTROL DESIGN

The control design is based on a detailed coupled MIMO plant model, which comprises the first order actuator model for each input channel and the rotor model. The rotor model is obtained using finite element modeling (FEM) [5]. The first three critical speeds of the rotor are 260, 539, and 952 Hz. The total rotor mass is 42.6 kg. The radial and axial suspensions are assumed decoupled and therefore they are considered separately. We consider the overall plant model in the state variable form as

$$\begin{aligned} \dot{\mathbf{x}} &= \boldsymbol{A}\mathbf{x} + \boldsymbol{B}\mathbf{u} + \boldsymbol{B}_{\mathrm{w}}\mathbf{w}, \\ \mathbf{y} &= \boldsymbol{C}\mathbf{x}, \end{aligned} \tag{1}$$

where $\boldsymbol{A}$, $\boldsymbol{B}$, $\boldsymbol{B}_{\mathrm{w}}$, $\boldsymbol{C}$, $\mathbf{x}$, $\mathbf{u}$, $\mathbf{w}$, and $\mathbf{y}$ are the state matrix, the input matrix, the disturbance input matrix, the output matrix, the state vector, the input vector, the disturbance input vector, and the output vector, respectively.

LQR and the Kalman filter

In the 'basic controller' without an UFRC, a linear quadratic regulator (LQR) and a state estimator (the Kalman filter) with additional constant disturbance observer are built as presented in [5].

The estimator is formed as

$$\begin{bmatrix} \dot{\bar{\mathbf{x}}} \\ \dot{\bar{\mathbf{w}}} \end{bmatrix} = \begin{bmatrix} \boldsymbol{A} & \boldsymbol{B}\boldsymbol{C}_{\mathrm{w}} \\ \mathbf{0} & \boldsymbol{A}_{\mathrm{w}} \end{bmatrix} \begin{bmatrix} \bar{\mathbf{x}} \\ \bar{\mathbf{w}} \end{bmatrix} + \begin{bmatrix} \boldsymbol{B} \\ \mathbf{0} \end{bmatrix} \mathbf{u} + \boldsymbol{L}(\mathbf{y} - \bar{\mathbf{y}}), \tag{2}$$

$$\bar{\mathbf{y}} = \begin{bmatrix} \boldsymbol{C} & \mathbf{0} \end{bmatrix} \begin{bmatrix} \bar{\mathbf{x}} \\ \bar{\mathbf{w}} \end{bmatrix}. \tag{3}$$

where $\bar{\mathbf{x}}$, $\bar{\mathbf{y}}$, and $\bar{\mathbf{w}}$ are the estimate of the state vector, the estimate of the output vector, and the estimate of the disturbance signal, respectively. We assume that the disturbances enter the plant inputs, and therefore the output matrix of disturbance model $\boldsymbol{C}_{\mathrm{w}}$ is unitary. The state matrix of constant disturbance $\boldsymbol{A}_{\mathrm{w}}$=**0**. However, for the optimal design of the estimator gain matrix $\boldsymbol{L}$ that provides satisfactory dynamics of estimation error, the system model (1) is augmented with the perturbed disturbance model. The perturbed disturbance model $\tilde{\boldsymbol{A}}_{\mathrm{w}}$ is diagonal with the elements roughly equal to the selected inverted integrator time constant. The estimator gain matrix $\boldsymbol{L}$ is obtained from the steady-state solution of the Riccati equation, based on the selection of output noise intensity and the process input noise intensity characteristics [5].

The state-feedback is formed by applying the feedback gain matrix $\boldsymbol{K}$ and the disturbance gain matrix $\boldsymbol{K}_{\mathrm{w}}$ as

$$\mathbf{u} = -\boldsymbol{K}\bar{\mathbf{x}} - \boldsymbol{K}_{\mathrm{w}}\bar{\mathbf{w}}. \tag{4}$$

The state-feedback controller gain matrix $\boldsymbol{K}$ minimizes the quadratic integral performance index J_{q}, that is

$$J_{\mathrm{q}} = \int_0^{\infty} \left[\mathbf{x}^{\mathrm{T}}\boldsymbol{Q}\mathbf{x} + \mathbf{u}^{\mathrm{T}}\boldsymbol{R}\mathbf{u}\right] dt, \tag{5}$$

where $\boldsymbol{Q}$, $\boldsymbol{R}$, $\mathbf{x}$, and t are the state weighting matrix, the control weight matrix, the state vector, and time. For determining the diagonal weighting matrices $\boldsymbol{Q}$ and $\boldsymbol{R}$ we utilize the Bryson's rules [6]. The disturbance gain matrix $\boldsymbol{K}_{\mathrm{w}}$=**I**.

Unbalance force rejection control

In the case of unbalance force cancellation, two different design methods are employed.

The first design generalizes the presented full state estimator with the constant disturbance estimate, as in (2)-(3), to the estimator that includes a sinusoidal disturbance model. The computation of the estimator gain matrix $\boldsymbol{L}$ is based on the augmented plant model, but with the perturbed state matrix of the disturbances

$$\tilde{\boldsymbol{A}}_{\mathrm{w}}' = \begin{bmatrix} \tilde{\boldsymbol{A}}_{\mathrm{w}} & \mathbf{0} & \mathbf{0} \\ \mathbf{0} & \mathbf{0} & \mathbf{I} \\ \mathbf{0} & \mathbf{I}\cdot\Omega^2 & \mathbf{I}\cdot 2\zeta\Omega \end{bmatrix}, \tag{6}$$

and with the output matrix of disturbance model

$$\boldsymbol{C}_{\mathrm{w}} = \begin{bmatrix} \mathbf{I} & \mathbf{I} & \mathbf{0} \end{bmatrix}. \tag{7}$$

where Ω and ζ are the rotational speed and the damping ratio of the sinusoidal disturbance model. The disturbance model is perturbed in order to utilize Matlab's Control Toolbox in the observer design. In particular, the negative damping ratio is assumed. This perturbation is introduced to move the roots of the augmented plant model from the imaginary axis. The resulting speed of the integration for the sinusoidal disturbance estimate is affected by the selection of the negative damping. For the implementation, the estimator is formed analogically to the one presented earlier without UFRC, where $\boldsymbol{A}_{\mathrm{w}}$=**0** and the damping ratio of the sinusoidal disturbance model equals zero. However, the disturbance gain matrix is

$$\boldsymbol{K}_{\mathrm{w}} = \begin{bmatrix} \mathbf{I} & \mathbf{I} & \mathbf{0} \end{bmatrix}. \tag{8}$$

The second design is based on the pole placement. It applies the closed-loop roots, which result from the Kalman filter design computed for the plant model (1), plus it adds the selected poles of the integrators. The integral poles are selected to be the same as the integral poles resulting from the first design.

In general, both a pole placement method and an optimal gain computation are equivalent. For both aforementioned design methods, when the plant model without the residual modes is applied, the resulting closed-loop poles are almost the same. However, the closed-loop pole patterns for the plant that includes the residual modes are different for both controllers. For the pole placement design, the residual modes are less damped than for the optimal design. Figure 1 presents the comparison of the singular value plots of the output sensitivity functions for the both controllers at Ω=5000 rpm.

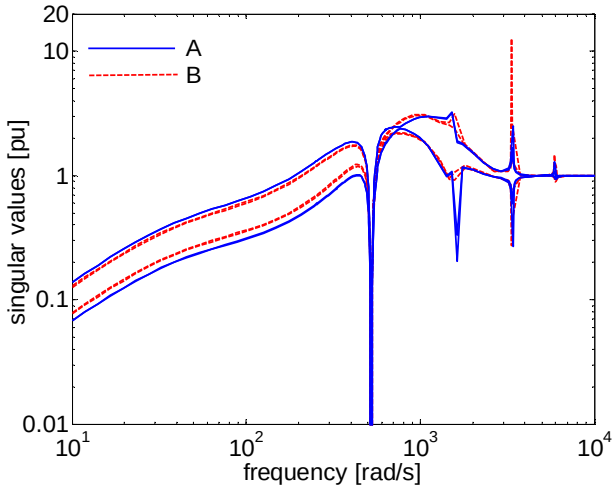

FIGURE 1: Singular values plot of the output sensitivity function for the control system with UFRC designed at Ω=5000 rpm = 523.6 rad/s.

The pole placement design (marked as B) is less robustly stable, in respect to the second flexible mode at 539 Hz, when compared to the optimal controller design (marked as A).

In the case of the magnetic force cancellation, the estimator gain matrix $\boldsymbol{L}$ is computed in the same manner as in the case of the unbalance force cancellation, but the sinusoidal disturbance estimate enters the estimator through the estimation error. The augmented plant model has the output equation such as

$$\bar{\mathbf{y}} = \begin{bmatrix} \boldsymbol{C} & \mathbf{0} & \mathbf{I} & \mathbf{0} \end{bmatrix} \begin{bmatrix} \bar{\mathbf{x}} \\ \bar{\mathbf{w}} \end{bmatrix}. \quad (9)$$

Moreover, only the constant disturbance estimate is used in a feedback. The disturbance gain matrix is

$$\boldsymbol{K}_{\mathrm{w}} = \begin{bmatrix} \mathbf{I} & \mathbf{0} & \mathbf{0} \end{bmatrix}. \quad (10)$$

Gain scheduling and implementation

For operation under a variable speed it is necessary to apply a gain scheduling to obtain an effective unbalance force rejection. In principle, the controllers with UFRC are designed by digital emulation. A design of each controller is done assuming the system to be continuous-time. Then a discrete equivalent of the controller is computed by using bilinear approximation and used in the place of the time-continuous controller. The number of controllers is calculated for the predefined vector of rotational speeds.

In the implementation, the vector of rotational speeds is used as a look up table (LUT) for selecting indices of the memory locations, which contain the pre-calculated controllers. Figure 2 shows the block diagram of the closed-loop system with the controller adapted according to the measured rotational speed.

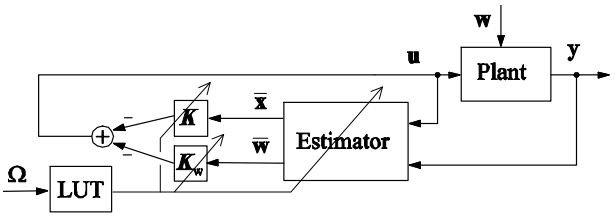

FIGURE 2: System with adaptive controller

EXPERIMENTAL INVESTIGATION

The experimental evaluations of the controller with an UFRC for the unbalance force cancellation and for the magnetic force cancellation are presented in Fig. 3 and in Fig. 4, respectively. The control current i_c and displacement from the rotor central position (x,y) at the heavier end of the rotor are measured. The heavier end of the rotor is referred here as an end-B.

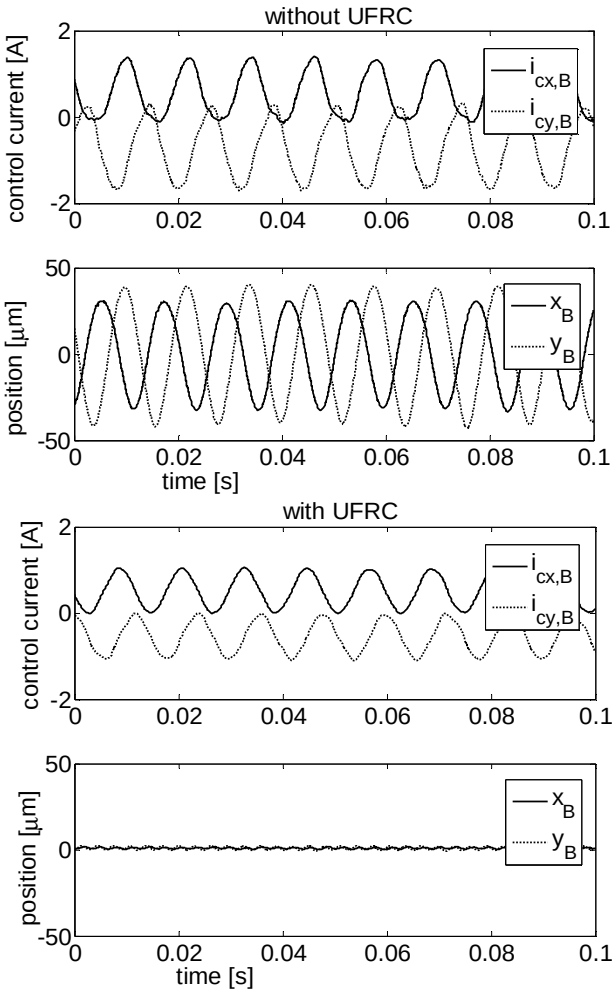

FIGURE 3: Measured system responses for the unbalance force cancellation when the couple unbalance is 500 g·mm and Ω=5000 rpm.

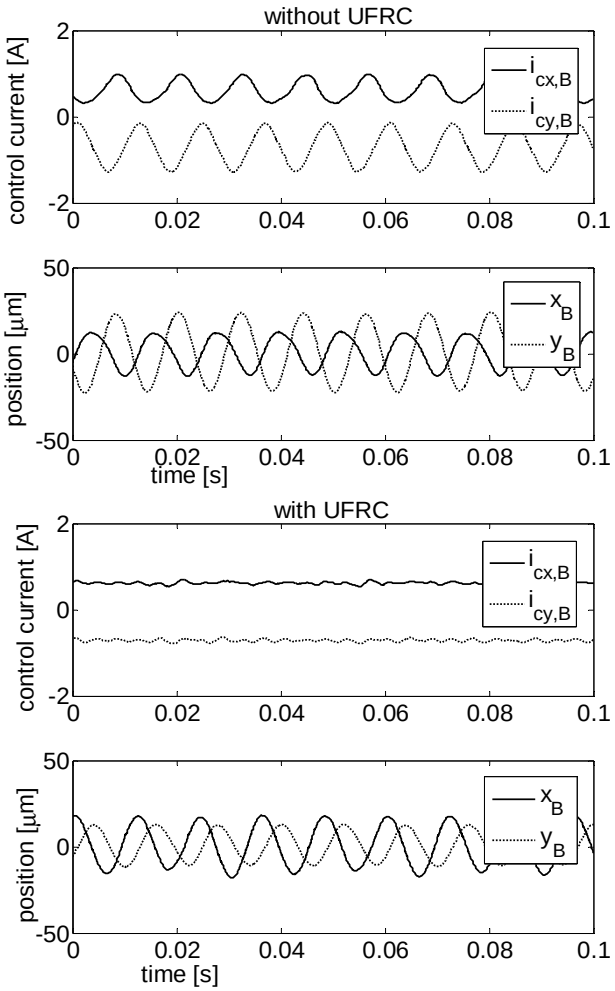

FIGURE 4: Measured responses of the system for the magnetic force cancellation when the couple unbalance is 250 g·mm and Ω=5000 rpm.

In fact, the rotor was not rotating, but the effect of couple unbalance, at the actuator nodes, was generated through the disturbance components in the control currents. The UFRC compensation required an accurate speed measurement (error up to 1-3 %) in order to work efficiently.

The experimental results are compared to the equivalent simulation results, which are presented for the unbalance force cancellation and for the magnetic force cancellation in Fig. 5 and Fig. 6, respectively. The simulation model comprises the detailed FEM based rotor model (as presented in [5]) with the first three flexible modes, the nonlinear actuator model with the force-field characteristics based on the reluctance network method (as presented in [7]), signal saturations, and the modulation delays.

The experimental results agree with the simulation results. However, in the experiment the force magnitudes acting on *x* and *y* axes are not equal. The possible reasons for this include, for example, working out of the operational point, inaccurate position measurements or their calibration.

The control designs with the gain scheduling according to the variable rotational speed are evaluated using simulations and the aforementioned high-order non-linear plant model. Figure 7 shows the changes of the rotor speed during the simulated acceleration of the rotor. Figure 8 presents the simulated responses of the system (control currents and displacement from the rotor central position) at the end-B of the rotor when there is no UFRC present. Figure 9 and Fig. 10 show the simulated responses of the system (control currents and displacement from the rotor central position) at the end-B of the rotor when there is UFRC applied for canceling the unbalance forces and for canceling the magnetic forces, respectively. UFRC with and without the gain scheduling scheme is considered. Only envelope curves of signal amplitudes are shown in Figs. 8-10.

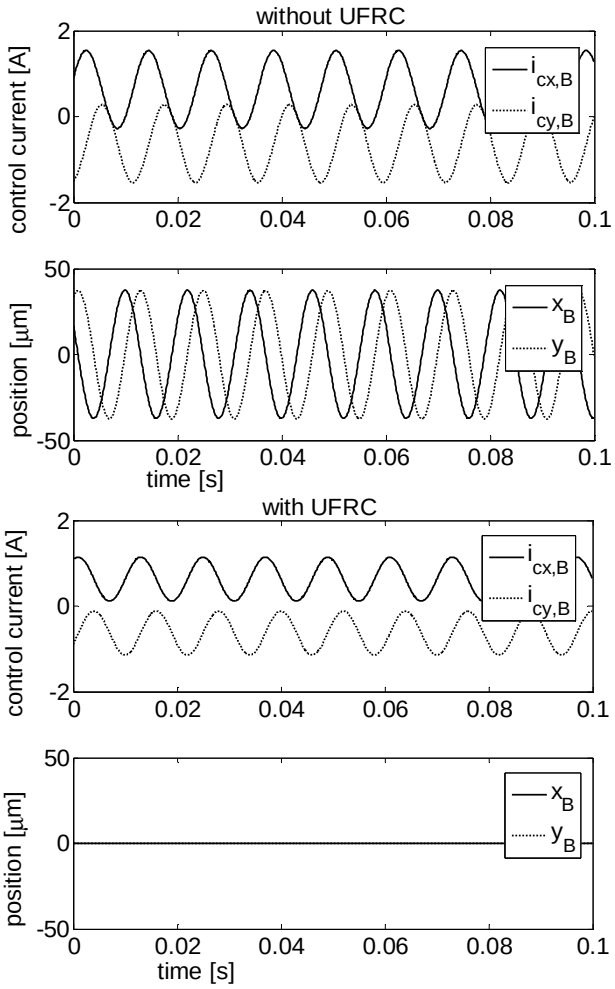

FIGURE 5: Simulated responses of the system for the unbalance force cancellation when the couple unbalance is 500 g·mm and Ω=5000 rpm.

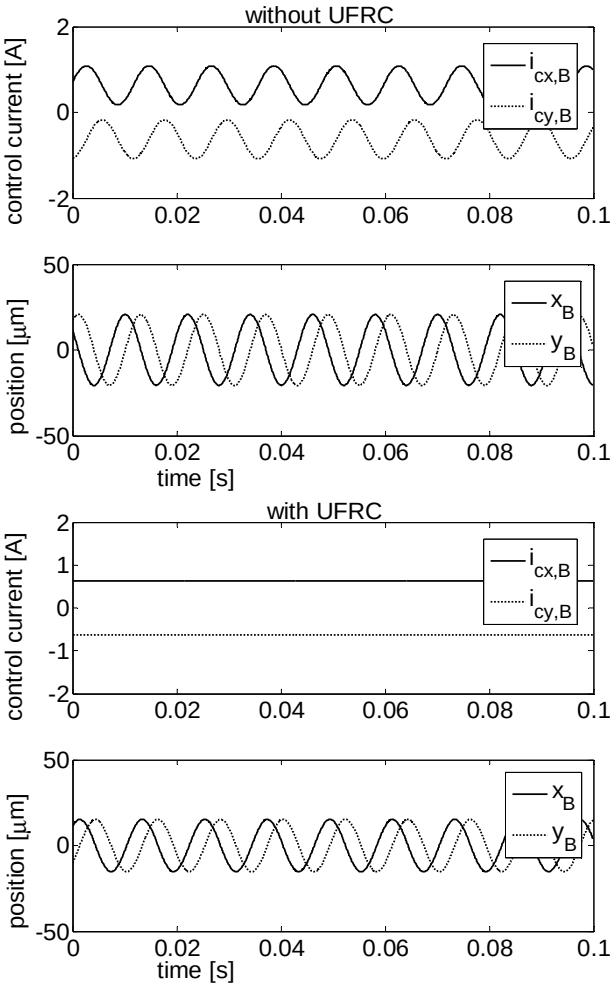

FIGURE 6: Simulated responses of the system for the magnetic force cancellation when the couple unbalance is 250 g·mm and Ω=5000 rpm.

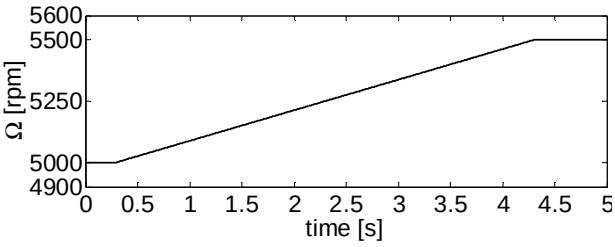

FIGURE 7: Variations of the rotational speed during the simulation.

Looking at Fig. 1 and Figs. 9-10, it is apparent that when there is no gain scheduling applied, the controller is only able to cancel the oscillations of frequencies close to that specific frequency for which it has been designed, that is Ω=5000 rpm.

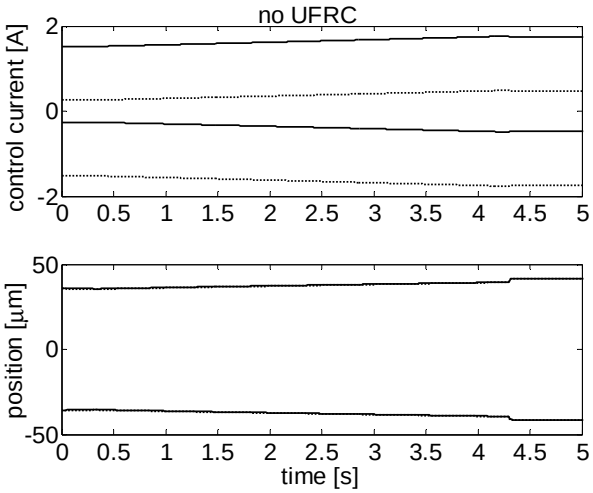

FIGURE 8: Simulated responses of the system when the couple unbalance is 500 g·mm and the rotor is accelerating.

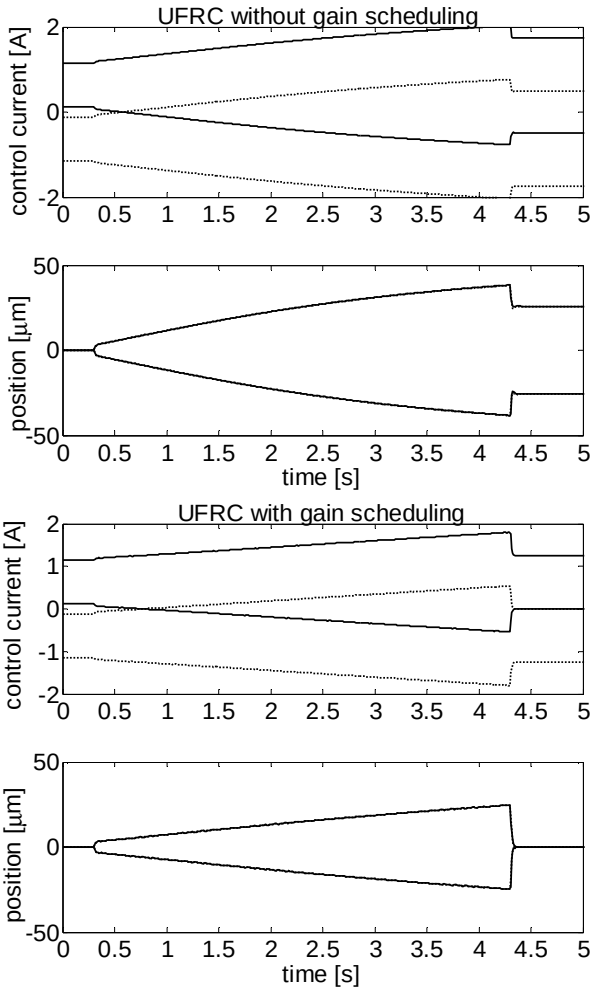

FIGURE 9: Simulated responses of the system with the unbalance force cancellation when the couple unbalance is 500 g·mm and the rotor is accelerating.

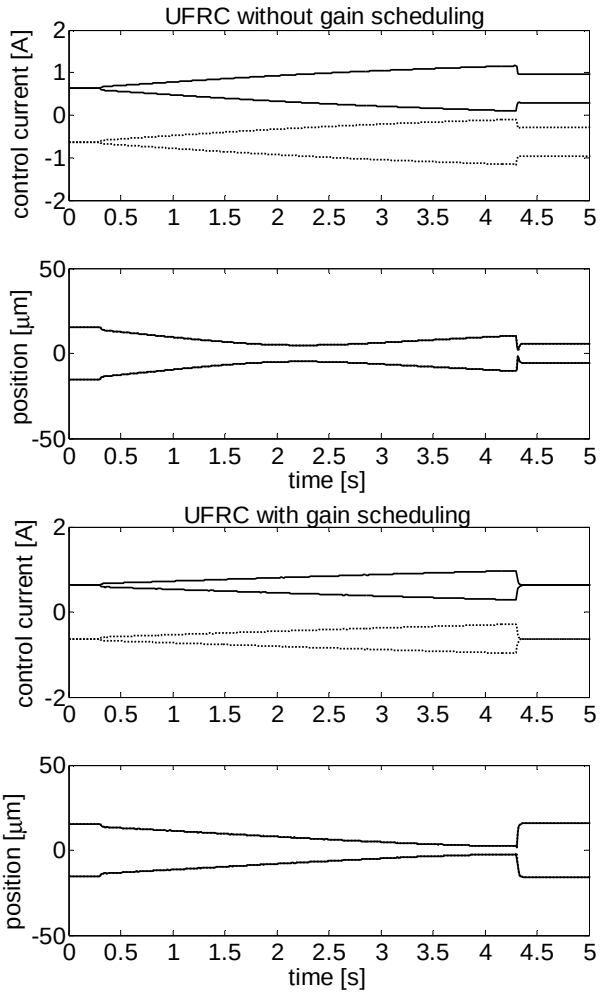

FIGURE 10: Simulated responses of the system with the magnetic force cancellation when the couple unbalance is 250 g·mm and the rotor is accelerating.

For the accelerating rotor, UFRC is in transient and cannot cancel vibrations as effectively as in the steady state. The sinusoidal vibrations excite also the constant disturbance estimator. However, the presence of the UFRC still improves the system responses during the tested acceleration when compared to the controller without an UFRC.

With gain scheduling, two strategies may be utilized. First, the gain scheduling mechanism and UFRC can be disabled when accelerating or decelerating and then activated when the rotor speed reaches the predefined speed. During the transient a controller without UFRC is active. In the second strategy, the gain scheduling mechanism and UFRC can be active all the time.

CONCLUSIONS

In this work, the full-order observer-based UFRC with the parameters scheduled according to the rotational speed is presented. The optimal controller with the UFRC could reject either unbalance forces or vibrations of magnetic forces.

In general, both a pole placement method and an optimal gain computation are equivalent when used for the design of UFRC. In the case of unbalance force cancellation, the pole placement method occurres to be less robustly stable than the optimal solution based on the perturbed disturbance model, with respect to the residual dynamics of the second flexible mode.

The applied gain scheduling provides the optimal UFRC for variable speed. This method requires an accurate speed measurements and a fair amount of memory for storing the controllers, which are designed for different rotational speeds.

References

[1] H. Bleuler, C. Gähler, R. Herzog, R. Larsonneur, T. Mizuno, R. Siegward, S. Woo, “Application of Digital Signal Processors for Industrial Magnetic Bearings”, Transactions on Control Systems Technology, vol. 2, no. 4, pp. 280-289, 1994.

[2] T.R. Grochmal, A.F. Lynch, “Vibration compensation and precision tracking of a rotating shaft by nonlinear state feedback”, in Proceedings of the Tenth International Symposium on Magnetic Bearings, CD-proceedings, 2006.

[3] K.-Y. Lum, V.T. Coppola, D.S. Bernstein, “Adaptive Autocentering Control for an Active Magnetic Bearing Supporting a Rotor with Unknown Mass Imbalance”, IEEE Transactions on Control Systems Technology, vol. 4, no. 5, pp. 587-597, 1996.

[4] E. Lantto, Robust Control of Magnetic Bearings in Subcritical Machines, Dissertation, Helsinki University of Technology, Finland, 1999.

[5] R. Jastrzębski, Design and Implementation of FPGA-based LQ Control of Active Magnetic Bearings, Dissertation, Lappeenranta University of Technology, Finland, 2007, available: http://urn.fi/URN:ISBN:978-952-214-509-3.

[6] G. F. Franklin, J. D. Powell, and M. Workman, Digital Control of Dynamic Systems, 3rd ed., Addison Wesley, 1998.

[7] J. Nerg, R. Pöllänen, and J. Pyrhönen, “Modelling the Force versus Current Characteristics, Linearized Parameters and Dynamic Inductance of Radial Active Magnetic Bearings Using Different Numerical Calculation Methods”, WSEAS Transactions on Circuits and Systems 4 (6): 551-559, 2005.